NEOPLASIA
www.neoplasia.com

Volume 14 Number 4 April 2012 pp. 297–310 297

The Ezrin Metastatic Phenotype Is Associated with the Initiation of Protein Translation[1]

Joseph W. Briggs*, Ling Ren*, Rachel Nguyen*, Kristi Chakrabarti*, Jessica Cassavaugh*, Said Rahim†, Gulay Bulut†, Ming Zhou‡, Timothy D. Veenstra‡, Qingrong Chen§, Jun S. Wei§, Javed Khan§, Aykut Uren† and Chand Khanna*

*Tumor and Metastasis Biology Section, Pediatric Oncology Branch, Center for Cancer Research, National Cancer Institute, Bethesda, MD, USA; †Lombardi Cancer Center, Georgetown University, Washington, DC, USA; ‡Laboratory of Proteomics and Analytical Technologies, Advanced Technology Program, SAIC – Frederick, Inc, National Cancer Institute - Frederick, Frederick, MD, USA; §Oncogenomics Section, Pediatric Oncology Branch, Center for Cancer Research, National Cancer Institute, Bethesda, MD, USA

Abstract

We previously associated the cytoskeleton linker protein, Ezrin, with the metastatic phenotype of pediatric sarcomas, including osteosarcoma and rhabdomyosarcoma. These studies have suggested that Ezrin contributes to the survival of cancer cells after their arrival at secondary metastatic locations. To better understand this role in metastasis, we undertook two noncandidate analyses of Ezrin function including a microarray subtraction of high- and low-Ezrin-expressing cells and a proteomic approach to identify proteins that bound the N-terminus of Ezrin in tumor lysates. Functional analyses of these data led to a novel and unifying hypothesis that Ezrin contributes to the efficiency of metastasis through regulation of protein translation. In support of this hypothesis, we found Ezrin to be part of the ribonucleoprotein complex to facilitate the expression of complex messenger RNA in cells and to bind with poly A binding protein 1 (PABP1; *PABPC1*). The relevance of these findings was supported by our identification of Ezrin and components of the translational machinery in pseudopodia of highly metastatic cells during the process of cell invasion. Finally, two small molecule inhibitors recently shown to inhibit the Ezrin metastatic phenotype disrupted the Ezrin/PABP1 association. Taken together, these results provide a novel mechanistic basis by which Ezrin may contribute to metastasis.

Neoplasia (2012) 14, 297–310

Introduction

Osteosarcoma (OS) is the most common primary tumor of bone. Despite effective control of the primary tumor and both neoadjuvant and adjuvant chemotherapy, the development of metastases to the lungs is the most common cause of death in OS patients. Furthermore, the long-term outcome for patients who present with metastatic disease is grave. The development of new and effective treatments based on a more thorough understanding of metastasis biology is needed.

Toward this end, we previously identified Ezrin as a protein associated with the metastatic phenotype of two highly metastatic pediatric cancers: rhabdomyosarcoma and OS [1,2]. Since then, Ezrin

Abbreviations: FERM, 4.1 Ezrin-Radixin-Moesin; MS-MS, tandem mass spectrometry; N-ERMAD, amino-terminal Ezrin, Radixin, Moesin association domain; UTR, untranslated region

Address all correspondence to: Chand Khanna, DVM, PhD, Tumor and Metastasis Biology Section, Pediatric Oncology Branch and Comparative Oncology Program, Center for Cancer Research, National Cancer Institute, National Institutes of Health, 37 Convent Dr, Rm 2144, Bethesda, MD 20892. E-mail: khannac@mail.nih.gov

[1]This article refers to supplementary materials, which are designated by Figures W1 and W2 and are available online at www.neoplasia.com.

Received 27 October 2011; Revised 13 March 2012; Accepted 16 March 2012

DOI 10.1593/neo.111518

expression has been linked to clinical outcome, clinical stage, or histologic grade in a number of cancers including mammary carcinoma, pancreatic carcinoma, cutaneous and uveal melanoma, uterine carcinoma, breast carcinoma, and soft tissue sarcoma [3–9]. Ezrin is a member of the ERM (Ezrin-Radixin-Moesin) protein family. Ezrin functions as a linker protein connecting the actin cytoskeleton (Ezrin C-terminus) to integral plasma membrane proteins (Ezrin N-terminus) [10,11]. Ezrin is proposed to exist in a dormant form in which the C-terminal tail binds to and masks the N-terminal FERM domain [12,13]. Therefore, amino-terminal Ezrin interactions are critical in determining not only the repertoire of proteins Ezrin can interact with but also the corresponding cellular functions that may be positively or negatively affected. This linkage to the cell membrane allows the cell to physically engage and potentially sense the tumor microenvironment. This linker function makes ERM proteins essential for many fundamental cellular processes, including the determination of cell shape, polarity and formation of surface structures, cell adhesion, motility, cytokinesis, phagocytosis, and integration of membrane transport with signaling pathways [14–17]. The linkage also leads to efficient signal transduction through membrane-associated proteins and receptors. In our previous studies of Ezrin and OS metastasis, we found that Ezrin was not constitutively phosphorylated but rather was dynamically regulated during metastatic progression [18]. Ezrin was phosphorylated early after cells arrived in the lung and again as they progressed into the lung microenvironment. Indeed, high Ezrin expression provided an advantage to highly metastatic cells during this time, resulting in the retention of greater cells in the lung compared with cells with low Ezrin expression. We hypothesize that Ezrin protects cells against apoptosis resulting from stresses faced by metastatic cells at critical periods during metastatic progression, namely early after cells arrive at secondary sites (Hong et al., unpublished observations). In addition and in support of this hypothesis, we recently identified two small molecule inhibitors that bind the N-terminus of Ezrin and inhibit the Ezrin-dependent metastatic phenotype [19]. However, the mechanism(s) by which Ezrin contributes to metastasis are still not understood.

To better define the role of Ezrin in metastasis, we undertook two noncandidate analyses of Ezrin protein function. First, we conducted complementary DNA (cDNA) microarray subtraction of high- and low-Ezrin-expressing tumor cells to identify differentially regulated genes, pathways, and processes. Microarray analysis revealed 124 genes with greater expression in high-Ezrin-expressing cells. Functional analysis of this transcriptional signature suggested that the process of protein translation, specifically translation initiation, was significantly associated with the Ezrin metastatic phenotype. Second, we used tandem mass spectrometry (MS-MS) analysis to identify proteins in tumor lysates that bound the N-terminus of Ezrin. Affinity chromatography and curation of MS-MS data identified 138 Ezrin-binding proteins. Functional analysis of these Ezrin-interacting proteins also revealed a link to the protein translation machinery. The surprising convergence of these noncandidate analyses of Ezrin function led to the hypothesis that Ezrin may contribute to the metastatic phenotype by modulating the efficiency of protein translation in tumor cells. Whereas there were no quantitative differences in total protein synthesis in high- and low-Ezrin-expressing cells, there was an Ezrin-dependent effect on the ability to translate a messenger RNA (mRNA) containing a structured 5′ untranslated region (UTR). As an explanation for this role, we found Ezrin interacts with the 3′ UTR binding protein, poly A binding protein 1 (PABP1; *PABPC1*), an association that has not been previously described. Furthermore, two Ezrin-binding small molecule inhibitors (NSC305787 and NSC668394) that decrease the Ezrin-dependent metastatic phenotype also inhibited Ezrin/PABP1 interaction. The relevance of these findings was supported by our identification of Ezrin and components of the translational machinery in cellular extensions of highly metastatic cells during the process of cell invasion. Taken together, our results linking Ezrin to the process of protein synthesis are novel and provide a new perspective for understanding how Ezrin contributes to the process of metastasis.

Materials and Methods

Cell Culture and Tissue Harvest

Characterization and maintenance of high-Ezrin/high-metastatic K7M2-WT, K7M2-neo (vector clone), intermediate-Ezrin/intermediate-metastasis AS13, and low-Ezrin/low-metastatic K12-WT, AS2.13, AS2.15, AS1.52, AS1.46 cells have been previously described [1,20]. Human OS (HOS-MNNG, U2 and 143B) and Ewing sarcoma (TC32) cell lines were maintained in Dulbecco modified Eagle medium (DMEM) supplemented with 10% fetal bovine serum, L-glutamine (2 mM), streptomycin (100 U/mL), and penicillin (100 U/mL; Invitrogen, Carlsbad, CA). Ezrin antisense clones were cultured in media containing G418 (Invitrogen). For affinity chromatography studies, K7M2 cells were grown to 80% confluence and harvested by trypsinization before injection to 4- to 6-week-old BALB/c mice by tail vein injection, as previously described [1]. The resultant pulmonary metastases in mice were dissected from surrounding lung and frozen for later use.

Plasmids and Transient Transfection Assays

The Ezrin N-ERMAD (Ezrin-Radixin-Moesin association domain) construct used for recombinant protein production has been previously described [21]. The Stem-Loop-luciferase reporter construct (pcDNA-SL-LUC) was kindly provided by Nancy Colburn [22]. For luciferase reporter assays, 5×10^5 cells were seeded on six-well plates in complete medium and transfected with 2.5 μg of pcDNA-SL-LUC using 7.5 μl of TransIT-LT1 reagent (Mirus, Madison, WI). Protein was harvested 24 or 48 hours after transfection. Firefly luciferase expression from pcDNA-SL-LUC was measured using the Luciferase Assay System (Promega, Madison, WI) in a Victor3 luminometer (PerkinElmer, Boston, MA).

Gene Silencing with Small Interfering RNA

The Ezrin small interfering RNA (siRNA) sequence was generously provided by Natasha Caplen from the Gene Silencing Section of the National Cancer Institute and manufactured along with a nonsilencing negative control by Qiagen Corporation (Valencia, CA). The Ezrin target sequence was 5′-CAGGACTGATTGAATTACGGA-3′ beginning at nucleotide 2149 of human Ezrin mRNA. The siRNA (50 nM final concentration) was added to cultured cells using siLentFect reagent (Bio-Rad, Hercules, CA). Ezrin suppression was verified using Western blot analysis.

Western Blot and Immunoprecipitation

Cells were lysed in either RIPA buffer (Upstate Biotechnology, Waltham, NY) plus protease and phosphatase inhibitor cocktail (Roche, Basel, Switzerland), 1× sodium dodecyl sulfate (SDS) or cell lysis buffer (Cell Signaling Technology, Danvers, MA). About 30 to 50 μg of protein was separated on Tris-glycine gels (Invitrogen) and transferred to nitrocellulose or polyvinylidene fluoride. The following

primary antibodies were used: eIF4E, ribosomal S6, ERM, phospho-ERM, PABP1, and YB-1 (Cell Signaling); β-actin and Ezrin (Sigma-Aldrich, St Louis, MO); RACK1, actinin, IQGAP1, annexin II, and RAN (BD Biosciences, Sparks, MD); CLIC4 and CLIC1 antibodies kindly provided by Dr Mark Berryman, Ohio University College of Osteopathic Medicine; and AHNAK and Rab14 provided by Dr Jacques Baudier, INSERM, Grenoble, France. Horseradish peroxidase–conjugated secondary antibodies and SuperSignal West Pico chemiluminescence substrate were used for detection (Pierce Biotechnology, Rockford, IL). For immunoprecipitation analysis, 24 hours after plating, cells were treated with 10 μM NSC305787 or NSC668394 for 5 hours in serum-free DMEM. Cells were lysed with buffer containing 50 mM HEPES, pH 7.9, 100 mM NaCl, 4 mM NaPP, 10 mM EDTA, 10 mM NaF, 1% Triton X-100, 2 mM sodium vanadate, 1 mM PMSF, 2 μg/ml aprotonin, 2 μg/ml leupeptin, and 1 μM calyculin A. Lysates were precleared with a 50% slurry of protein G agarose resin and incubated overnight with 2 μl of Ezrin antibody (no. E8897; Sigma-Aldrich). Antigen-antibody complexes were selected with protein G agarose beads, washed three times, and analyzed by SDS-PAGE.

cDNA Microarray Procedure

Total RNA was extracted from eight murine OS cell lines (K7M2-WT, K7M2-neo, AS13, AS2.13, AS2.15, AS1.52, AS1.46, and K12) for cDNA microarray experiments; RNA preparation and microarray experiments were done as previously described [23]. The RNA obtained from K7M2-neo (high-Ezrin transfection control) was used as a reference (Cy3 labeled) in all two-color cDNA microarrray experiments. Data normalization and principal component analysis were performed as previously described [23,24]. The normalized expression ratios of experiments (seven cell lines) *versus* control (high-Ezrin control K7M2-neo) for this filtered list were obtained for further analyses. Two criteria were used to identify genes of interest. First, we selected the cDNAs with a mean expression ratio of 0.7 to 1.3 in the high-Ezrin group. From this list of cDNAs, only those with a mean expression ratio of greater than 2 or less than 0.5 in the low-Ezrin group were then selected. These filtering steps yielded 181 cDNAs of interest, which were then analyzed by hierarchical clustering using Cluster software version 3.0 (Tokyo University, Tokyo, Japan). The heat map was generated using Java TreeView1.0.8 (http://jtreeview.sourceforge.net). Expression analysis systematic explorer (EASE) analysis was performed as previously described [25]. In addition, BLAST2GO (http://www.blast2go.org) was used to determine overrepresented GO terms attributed to Ezrin-interacting proteins identified by affinity chromatography and MS-MS identification [26]. Quantitative polymerase chain reaction analysis of select differentially expressed genes was performed using total cellular RNA. Primers were custom designed and synthesized by Invitrogen, and sequences are available on request.

Ezrin N-ERMAD Affinity Chromatography

The generation and purification of recombinant Ezrin N-ERMAD protein and purification have been described previously [27]. Metastatic lung nodules were grossly dissected into pieces no larger than 2 × 2 mm, weighed and suspended in cold extraction buffer (50 mM Tris, pH 7.4, 150 mM NaCl, 1 mM EDTA, 0.1% Triton X-100 protease inhibitors) at 5 ml/g of tissue. The tissue was homogenized, sonicated, and centrifuged at 50,000*g* for 30 minutes, followed by ultracentrifugation at 200,000*g* for 30 minutes. Ten milliliters of tumor protein extract (5 mg/mL) was incubated with 100 μl of Ezrin N-ERMAD or BSA-coated sepharose beads. Soluble Ezrin N-ERMAD protein was added to selected reactions for competition. Samples were incubated overnight at 4°C, washed eight times with cold TBS/0.1% Triton X-100, and bound proteins eluted by boiling in 2× SDS sample buffer.

Tandem Mass Spectrometry

After affinity chromatography as described, protein bands were excised and subsequently subjected to in-gel tryptic digestion to extract peptides [28]. Each peptide sample was desalted, lyophilized, and resuspended in 0.1% formic acid for liquid chromatography–MS-MS analysis using an Agilent 1100 capillary high-performance liquid chromatography system (Agilent Technologies, Santa Clara, CA) with a 10-cm integrated micro reverse phase liquid chromatography–electrospray ionization emitter column, coupled online with a LCQ Deca XP mass spectrometer (Thermo Fisher Scientific, Fair Lawn, NJ). Peptides were eluted using a linear gradient of 2% mobile phase B (acetonitrile with 0.1% formic acid) to 42% mobile phase B. The ion trap-mass spectrometer was operated in a data-dependent MS-MS mode in which the three most intense peptide molecular ions in the MS scan were sequentially and dynamically selected for subsequent collision-induced dissociation using a normalized collision energy of 35%. The mass spectra were acquired at the mass range of *m/z* 475 to 2000. The ion-source capillary voltage and temperature were set at 1.7 kV and 180°C, respectively. The MS-MS data were used to search the EBI UniProt *Homo sapiens* database (http://www.ebi.ac.uk/integr8). Up to two missed cleavage sites were allowed during the database search. The cutoff for legitimate identifications were charge state–dependent cross-correlation (X_{corr}) ≥ 2.0 for $[M + H]^{1+}$, ≥2.5 for $[M + 2H]^{2+}$, and ≥3.0 for $[M + 3H]^{3+}$ with delta correlation (ΔC_n) ≥ 0.10. Additional protein identification was carried out on a 4800 matrix-assisted laser desorption/ionization-tandem time of flight (MALDI-TOF-TOF) analyzer (Applied Biosystems, Carlsbad, CA) in reflector-positive mode and then validated in MS-MS mode. Select MS-MS–identified Ezrin-interacting proteins were identified by subtracting nonspecific interactors by subtracting peptides found to interact with BSA and then for proteins not represented by two or more peptides in the MS-MS data. Detected peptides were then prioritized for assessment based on actual versus predicted molecular weight (MW) and peptide coverage. Proteins with a MW observed/actual between 0.7 and 1.5 were selected.

m7-GTP Cap Affinity Binding Assay

Cells were grown to ~50% confluence and lysed, and the supernatant was precleared with 50 μl of sepharose CL-4B beads (50/50 slurry in wash buffer 1). Samples were centrifuged and supernatant transferred to a new tube where 50 μl of m7-GTP sepharose beads (GE Lifesciences, Piscataway, NJ) were added. Negative control reactions received sepharose CL-4B beads without m7-GTP coating. Samples were washed twice with wash buffer 1 (20 mM Tris-HCl, pH 7.5, 150 mM NaCl, complete protease, and phosphatase inhibitors) and once with wash buffer 2 (20 mM Tris-HCl, pH 7.5, 300 mM NaCl, complete protease, and phosphatase inhibitors). Bound protein was eluted with 2× SDS sample buffer with heating.

Polysome Analysis by Sucrose Density Gradient Fractionation

Cells were grown in complete DMEM and harvested at ~50% confluence. Immediately before harvesting, cells were incubated with

cycloheximide (200 μg/ml) for 10 minutes at 37°C. Samples were then placed on ice and washed twice with ice-cold PBS. Cells were then lysed in polysome lysis buffer (250 mM KCl, 10 mM Tris-HCl, pH 7.4, 25 mM $MgCl_2$, 0.5% NP-40, 0.5% sodium deoxycholate, 1 μg/μl RNasin, 200 μg/ml cycloheximide, EDTA-free protease inhibitors [Roche, Indianapolis, IN], phosphatase inhibitors, and nuclease-free water) and incubated on ice for 15 minutes followed by centrifugation at 4°C for 10 minutes at 12,000*g*. EDTA (25 mM final concentration) was added to the lysis buffer in place of Mg^{2+} for control samples to disrupt ribosomes. Supernatant was layered on 15% to 45% (wt/vol) sucrose gradients and centrifuged at 180,000*g* for 2.5 hours at 4°C. An ISCO Model 640 fractionator with a UV-6 absorbance monitor, 10-mm path-length flow cell, was used to measure the optical density of the gradients at 254 nm in real time. A Dataq model DU-158 analog-to-digital converter was used for data acquisition using Windaq software (Dataq Instruments, Akron, OH).

Enzyme-Linked Immunosorbent Assay

ELISA experiments were performed by coating a 96-well high-protein-binding ELISA plate (M0661; Sigma) with 200 ng of recombinant Ezrin protein. Nonspecific binding sites were blocked with 4% bovine serum albumin for 2 hours at room temperature. Five hundred micrograms of total protein from K12-WT cell lysate was added and incubated for 2 hours at room temperature. PABP1 bound to Ezrin was detected using a PABP1 antibody (no. ab6125; Abcam, Cambridge, MA) and a horseradish peroxidase–conjugated antimouse antibody (Sigma-Aldrich). Finally, 2,2′-azino-di-3-ethyl-benzthiazline sulfonate (Sigma-Aldrich) substrate was added, and the optical density at 405 nm was measured after 15 minutes.

Protein Isolation from Pseudopodia and Cell Bodies

Protein was isolated from migrating pseudopodia ("feet") and cell bodies using the Pseudopodia Purification Kit (Chemicon International, Temecula, CA) according to manufacturer's instructions.

Results

Microarray Analysis Defines an Ezrin-Dependent Gene Expression Signature

To define the Ezrin-associated metastatic phenotype at the level of transcription, cDNA microarray subtraction of high- and low-Ezrin-expressing OS cell lines was carried out. Three cell line clones with high Ezrin expression, three with low Ezrin expression and one with intermediate Ezrin expression were hybridized with the high-Ezrin transfection control, K7M2-neo, in two-color cDNA microarray experiments. One hundred eighty-one (181) genes were differentially expressed (*vs* the high-Ezrin control) with 57 downregulated and 124 upregulated (Figure 1). As predicted, AS13, the cell line with intermediate Ezrin levels showed intermediate expression (between high- and low-Ezrin cell lines) of the 181 genes of interest. Characterization of differentially expressed genes, based on non–mutually exclusive gene ontology (GO) function assignment, was conducted using EASE analysis. It revealed several specific gene functions significantly overrepresented in the 181 genes of interest compared with the total gene set of non–differentially expressed transcripts. Functions such as development, microtubule cytoskeleton, cytoskeleton, and microtubule-associated complex were expected based on existing knowledge of Ezrin biology (Table 1). However, other functions were unexpectedly found to correlate with Ezrin expression. For example, an area of biologic interest not previously associated with Ezrin activity but highly overrepresented in our analysis was protein translation. Translation, translation initiation, and translation initiation factor activity were

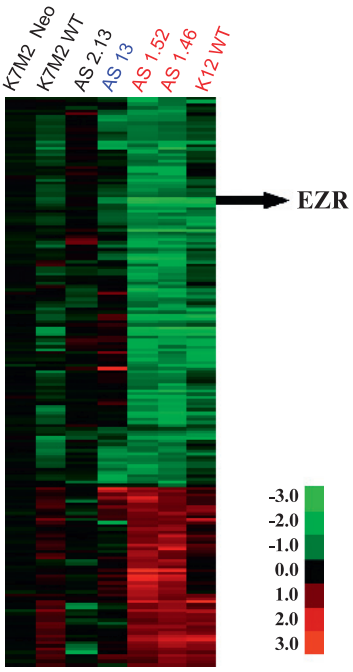

Figure 1. Hierarchical clustering of 181 differentially expressed cDNAs define the Ezrin phenotype. A 21k cDNA microarray subtraction of high (K7M2 WT, and AS 2.13), intermediate (AS13), and low (AS 1.52, AS 1.46, and K12 WT) compared with a high-Ezrin control (K7M2-neo). High-Ezrin-expressing cell lines (black) show little to no difference in expression ratios compared with K7M2-neo, whereas low-Ezrin-expressing cell lines (red) show marked differences in expression. The intermediate-Ezrin-expressing cell line, AS 13, falls predictably between the high- and low-Ezrin expression ratios. Expression differences from select microarray outliers were validated at the protein level and by polymerase chain reaction (data not shown). Characterization of 181 differentially expressed genes, based on non–mutually exclusive GO function assignment, was conducted using EASE (Table 1).

Table 1. Functions That Define the Ezrin Microarray Transcription Phenotype Ranked by EASE Score.

GO Function	EASE Score*	Fisher Exact *t* Test
Development	1.89*e* – 02	3.53*e* – 02
Microtubule cytoskeleton	3.09*e* – 02	2.21*e* – 02
Endopeptidase activity	3.77*e* – 02	1.49*e* – 02
Cytoskeleton	4.52*e* – 02	6.52*e* – 02
Microtubule-associated complex	6.98*e* – 02	4.52*e* – 02
Translation initiation	7.30*e* – 02	4.70*e* – 03
Neuron differentiation	7.64*e* – 02	1.00*e* – 04
Polyamine metabolism	1.23*e* – 01	2.00*e* – 04
Translation	1.03*e* – 01	3.93*e* – 02
Translation initiation factor activity	1.05*e* – 01	1.52*e* – 02
Morphogenesis	1.11*e* – 01	1.33*e* – 01
Kinesin complex	1.21*e* – 01	8.37*e* – 02
Learning and/or memory	1.36*e* – 01	1.50*e* – 03
Peptidase activity	1.41*e* – 01	1.35*e* – 01
RNA binding	1.41*e* – 01	1.35*e* – 01

*The value or EASE score is based on sliding Fisher exact probabilities where an EASE score of less than 1.0 suggests overrepresentation of a function. The 15 functions with the lowest scores are listed.

overrepresented GO functions that were associated with the following four genes: *eIF4e*, *Ormdl2*, *eIF3S4*, and *eIF1AY*. The increase in eIF4e expression in high-Ezrin cell lines, K7M2-wt and K7M2-neo, has been confirmed by Western blot (C. Khanna, unpublished observations, personal communication). This functional approach to the analysis of our microarray data suggested the hypothesis that Ezrin expression was associated with altered regulation of the translation machinery in these OS cells.

Ezrin Affinity Chromatography Independently Identifies Proteins Involved in Translation

In parallel to the microarray studies described, a noncandidate proteomic-based evaluation of Ezrin included the identification of Ezrin-binding proteins, using affinity chromatography followed by MS-MS. The amino (N) terminus of Ezrin has previously been shown to be involved in numerous protein-protein interactions while the carboxy (C) terminus primarily binds actin. In addition, the C-terminus of activated Ezrin primarily binds f-actin, whereas the diversity of Ezrin N-terminal interactions is far greater. Therefore, we chose to use the N-terminus for affinity chromatography experiments to "capture" Ezrin-interacting proteins from OS tumor lysates. The proteins identified using MS-MS were prioritized to eliminate those proteins that nonspecifically bound to BSA and were not identified by multiple unique peptides in the MS-MS data (Figure W1). This filtering algorithm yielded 138 proteins that bound Ezrin with strong coverage in OS tumor lysates (Table 2). Western blot analysis of selected proteins eluted from N-Ezrin sepharose beads validated the MS-MS identification of putative Ezrin-interacting proteins (Figure W2). Disruption of the actin cytoskeleton in the harvested protein lysates using latrunculin B demonstrated the requirement of actin for the observed interactions between most candidate proteins and Ezrin (suggestive of indirect protein interactions with Ezrin). RACK1, the protein translation-associated scaffolding protein, and, to a lesser extent, Rab-14, the large GTPase trafficking protein, demonstrated persistent strong elution from N-Ezrin beads after actin disruption. A direct interaction between RACK1 and Ezrin could not be demonstrated by coimmunoprecipitation with available antibodies. Functional classification of the 138 direct and indirect Ezrin-binding proteins included GO terms for membrane trafficking and cytoskeleton that were expected based on known functions of Ezrin (Table 3). In addition, proteins associated with translation and translation initiation were also enriched, including YB-1 (Y-box binding protein 1), RACK1 (receptor for activated C-protein kinase), and several eukaryotic translation initiation and elongation factors. To the best of our knowledge, Ezrin has not previously been shown to interact directly or indirectly with these proteins or to be associated with the process of protein synthesis. Taken together, the results from both noncandidate genomic and proteomic studies suggested a novel link between Ezrin and the process of protein translation.

Functional Analysis of the Translation Machinery in OS Cells

Next, to determine the extent to which Ezrin expression correlated with changes in global translation, we used sucrose density gradient centrifugation to analyze and quantify polysome profiles from high- and low-Ezrin-expressing cells. This approach allowed for quantification of total protein and mRNA associated with free messenger ribonucleoprotein complexes (mRNPs), individual ribosomal subunits (40S and 60S), monosomes (80S), and actively translating polysomes (mRNA containing more than two 80S particles). A global increase in translation initiation would be expected to result in an increase in the A_{254} signal intensity for the heavy polysome fractions (areas of active protein translation). Quantification of the area under the peak for fractions 8 to 20 (containing more than two ribosomes) revealed no difference between the high- and low-Ezrin-expressing cell lines, suggesting similar rates of global translation (Figure 2*A*). Cells treated with thapsigargin, a well-characterized inhibitor of translation initiation, demonstrated an expected shift in polysome profiles in both cell lines. Given the similarities in global translational rates, we hypothesized that differences may exist in the efficiency of translation of specific mRNA, namely those containing complex 5′UTR (Figure 2*B*). mRNA with complex 5′UTR have been shown to be "weakly" translated compared with the majority of other mRNA species. Numerous proto-oncogenes and antiapoptotic genes possess 5′UTRs that may form complex secondary structures. The rate-limiting step in synthesizing peptides from these messages seems to be during assembly of the preinitiation complex or initiation [29–32]. To model the expression of such complex 5′UTRs, we expressed a luciferase reporter with a hairpin/loop structure (δG = –44.8 kcal/mol) placed upstream of a luciferase protein coding sequence in cells with high and low Ezrin (Figure 2*B*). This stem-loop sequence was previously shown to dramatically inhibit protein synthesis of the downstream cistron [22]. Cells with more efficient translational machinery would be expected to better translate the stem-loop reporter mRNA resulting in increased luciferase activity. Indeed, cells with high Ezrin were able to express this complex synthetic (weakly translated) reporter more efficiently than cells in which Ezrin was suppressed. A similar correlation in stem-loop luciferase activity was seen after siRNA-mediated knockdown of Ezrin expression in human OS (HOS-MNNG, U2OS, 143B), rhabdomyosarcoma (Rh30), and Ewing sarcoma (TC32) cell lines (data not shown). Taken together, these results suggest that Ezrin expression specifically correlates with an increase in the ability to express an mRNA with a complex 5′UTR, without changes to overall protein synthesis.

To provide an explanation for how Ezrin contributes to the initiation of protein translation, we analyzed OS cell lysates, again by sucrose density gradient centrifugation, to determine the extent to which Ezrin protein was present in fractions containing complete, intact ribosomes (80S monomers) as well as actively translating polysomes (Figure 3*A*). Western blot analysis of Ezrin and previously identified proteins linked to translation was conducted on protein isolated from each fraction. As shown in Figure 3*A*, PABP1 and RACK1 were found in fractions containing ribosomal subunits, monosomes, or polysomes and undetectable in the free mRNP fractions. This is consistent with previous reports of RACK1 as a core ribosome-binding protein and PABP1's role in binding the poly A tail of mRNA as part of the protein translation complex [33,34]. eIF4E was detected mainly in fractions containing free mRNPs and 40S-80S complexes consistent with its role in translation before initiation. YB-1 was enriched in polysome fractions consistent with its role as an mRNA binding protein involved in regulating translation [35]. Ezrin was detected primarily in free mRNP fractions as well as fractions corresponding to 40S, 60S and 80S particles (Figure 3*A*). However, Ezrin was not detected in high-MW polysomes. Using an antibody that detects the ERM (Ezrin, Radixin, Moesin) family members, including Ezrin, a similar pattern of protein detection was seen (data not shown). These results suggest that several functional pools of Ezrin may be present and that Ezrin detected in fractions containing eIF4E, RACK1, PABP1, and/or YB-1

Table 2. List of Ezrin N-ERMAD Interacting Proteins Identified by Affinity Chromatography and Tandem Mass Spectrometry.

Annotation	Accession*	Length (aa)	Peptide† Matches	Score‡
Ezrin (p81) (Cytovillin) (Villin 2)	P15311	586	242	2.42
Tropomyosin 1 alpha chain	P09493	284	68	4.18
DNA-binding protein A (NF-GMB)	P16989	372	66	5.64
Moesin	P26038	577	86	6.71
Annexin A2 (Annexin II)	P07355	339	48	7.06
RACK1	P25388	317	41	7.73
Nucleolin (protein C23)	P19338	707	81	8.73
PCNA/cyclin	P12004	261	28	9.32
NAC alpha	Q13765	215	22	9.77
YB-1 (CBF-A)	P16991	324	29	11.17
ADP-ribosylation factor 1	P32889	181	16	11.31
RAN (Ran GTPase)	P17080	216	19	11.37
Four and a half LIM domains protein 1 (FHL-1)	Q13642	323	24	13.46
H326 protein	Q12839	597	43	13.88
TLS-associated serine-arginine protein 1	Q96G09	173	12	14.42
EF-hand domain protein 2/Swiprosin 1	Q96C19	240	14	17.14
EBP50/NHERF-1	O14745	358	20	17.90
Radixin	P35241	583	32	18.22
Thrombospondin 1 precursor	P07996	1170	62	18.87
Desmin	P17661	470	24	19.58
Tropomyosin alpha 3 chain (tropomyosin 3)	P06753	284	14	20.29
Protein C14orf166 (CGI-99)	Q9Y224	244	12	20.33
Calsequestrin	P31415	390	18	21.67
Eukaryotic initiation factor 4A-I (eIF4A-I)	P60842	406	18	22.56
Thioredoxin-like protein (32 kDa)	O43396	289	12	24.08
Leucine-zipper protein FKSG13	Q9HAP4	390	16	24.38
TCP-1-alpha (CCT-alpha)	P17987	556	22	25.27
Calgizzarin (S100C protein)	P31949	105	4	26.25
ADP-ribosylation factor-like protein 1	P40616	181	6	30.17
E3KARP/NHERF-2	Q15599	337	11	30.64
Ribose-phosphate pyrophosphokinase II	P11908	318	9	35.33
TCP-1-beta (CCT-beta)	P78371	535	15	35.67
Polyadenylate binding protein 1 (PABPC1)	P29341	636	17	37.41
ARP2/3 complex 16 kDa subunit (p16-ARC)	O15511	151	4	37.75
Tropomyosin beta-chain (Tropomyosin 2)	P07951	284	7	40.57
C-rich secretory protein-3 precursor (CRISP-3)	P54108	245	6	40.83
Ras-related protein Rab-18	Q9NP72	206	5	41.20
Clathrin coat assembly protein AP50 (AP50)	P20172	435	10	43.50
Lamin A/C (70 kDa lamin)	P02545	664	15	44.27
Calcyclin	P06703	90	2	45.00
Ribose-phosphate pyrophosphokinase I	P60891	318	7	45.43
GTP-binding protein Rheb	Q15382	184	4	46.00
alpha-centractin (Centractin)	P61163	376	8	47.00
Clathrin coat assembly protein AP17 (AP17)	P53680	142	3	47.33
CapZ alpha-1	P52907	286	6	47.67
TCP-1-theta (CCT-theta)	P50990	548	11	49.82
Ras-related protein Rab-10	P61026	200	4	50.00
Eukaryotic initiation factor 4A-II (eIF4A-II)	Q14240	407	8	50.88
Ras-related protein Rab-2A	P61019	212	4	53.00
Ras-related protein Rab-14	P61106	215	4	53.75
Ubiquitin thiolesterase protein OTUB1	Q96FW1	271	5	54.20
S/T protein phosphatase PP1-alpha 1 catalytic	P08129	330	6	55.00
GRP 78	P11021	654	11	59.45
Chloride intracellular channel protein 1 (CLIC1)	O00299	241	4	60.25
Caspase-14 precursor (CASP-14)	P31944	242	4	60.50
Selenoprotein H	Q8IZQ5	122	2	61.00
PDZ-LIM protein mystique	Q9H4L9	366	6	61.00
eIF-6 (B4 integrin interactor)	P56537	245	4	61.25
Ras-related protein Rap-1A	P10113	184	3	61.33
14-3-3 protein eta	Q04917	247	4	61.75
26S protease regulatory subunit 7	P35998	433	7	61.86
Tropomyosin TPMsk3 (Fragment)	CAH71266	248	4	62.00
NHP2-like protein 1	P55769	128	2	64.00
Adenylate kinase isoenzyme 1	P00568	194	3	64.67
TCP-1-delta (CCT-delta)	P50991	539	8	67.38
TCP-1-epsilon (CCT-epsilon)	P48643	541	8	67.63
Ras-related protein Rab-1A	P11476	205	3	68.33
Ras suppressor protein 1 (Rsu-1)	Q15404	277	4	69.25
CapZ alpha-2	P47755	286	4	71.50
GTP-binding protein Rit1	Q92963	219	3	73.00
26S protease regulatory subunit 6A	P17980	439	6	73.17
C6.1A protein	P46736	316	4	79.00
Sideroflexin 3	Q9BWM7	321	4	80.25

Table 2. (*continued*)

Annotation	Accession*	Length (aa)	Peptide† Matches	Score‡
Vacuolar ATP synthase subunit H	Q9UI12	483	6	80.50
14-3-3 protein tau	P27348	246	3	82.00
14-3-3 protein zeta/delta	P29312	246	3	82.00
TCP-1-eta (CCT-eta)	Q99832	543	6	90.50
DNA replication licensing factor MCM5	P33992	734	8	91.75
CapZ beta	P47756	277	3	92.33
Peroxisomal membrane protein PEX14	O75381	377	4	94.25
Rho-related GTP-binding protein RhoG	P35238	191	2	95.50
p21-Rac1 (Ras-like protein TC25)	P15154	192	2	96.00
GRP 75 (stress-70 protein, mitochondrial)	P38646	679	7	97.00
SAR1a (COPII-associated small GTPase)	Q9NR31	198	2	99.00
ARP2/3 complex 34 kDa subunit (P34-ARC)	O15144	300	3	100.00
(SERCA1) (SR Ca(2+)-ATPase 1)	O14983	1001	10	100.10
Ras-related protein Rab-35 (Rab-1C)	Q15286	201	2	100.50
26S proteasome non-ATPase reg. subunit 2	Q13200	908	9	100.89
26S protease regulatory subunit 8	P47210	406	4	101.50
Ras-related protein Rab-11A (Rab-11)	P24410	216	2	108.00
S/T PP2A, subunit B, B-alpha isoform (55 kDa)	Q00007	447	4	111.75
alpha-1 catenin	P35221	906	8	113.25
alpha-actinin 4	O43707	911	8	113.88
Ras-related protein Rab-33B	Q9H082	229	2	114.50
S/T protein PP2A, subunit A, PR65-alpha	P30153	589	5	117.80
14-3-3 protein gamma	P35214	248	2	124.00
Chloride intracellular channel protein 4 (CLIC4)	Q9Y696	253	2	126.50
Interleukin enhancer binding factor 2, 45 kDa	CAI18796	390	3	130.00
Putative GTP-binding protein PTD004	Q9NTK5	396	3	132.00
GRP94 (endoplasmin tumor rejection antigen 1)	P14625	803	6	133.83
Signal recognition particle receptor beta-subunit	Q9Y5M8	271	2	135.50
Euk. Transl. Init. factor 3 subunit 6 (eIF-3e, p48)	P60228	445	3	148.33
Cell division control protein 2 homolog (CDK1)	P06493	297	2	148.50
GABA(A) receptor	Q8N1C3	465	3	155.00
Fragile X MRRP-1	P51114	621	4	155.25
Protein kinase, interferon-inducible	NP_003681	313	2	156.50
Protein C14orf120	Q8NEJ9	315	2	157.50
Protein arginine *N*-methyltransferase 5	O14744	637	4	159.25
Interferon-induced 56 kDa protein (IFI-56K)	P09914	478	3	159.33
Sideroflexin 1	Q9H9B4	322	2	161.00
Mitotic checkpoint protein BUB3	O43684	328	2	164.00
Fascin (55 kDa actin bundling protein) (p55)	Q16658	493	3	164.33
AH receptor-interacting protein (AIP)	O00170	330	2	165.00
Serine hydroxymethyltransferase (SHMT)	P34897	504	3	168.00
Annexin A1 (Annexin I)	P04083	346	2	173.00
TCP-1-zeta-2 (CCT-zeta-2)	Q92526	530	3	176.67
26S proteasome non-ATPase reg. subunit 3 (p58)	O43242	534	3	178.00
Euk. Transl. Init. factor 3 subunit 6 interacting protein (HSPC021/HSPC025)	Q9Y262	564	3	188.00
cAMP-PK type I-alpha regulatory chain (TSE1)	P10644	381	2	190.50
Rev interacting protein Rip-1	Q13601	381	2	190.50
β-Catenin (PRO2286)	P35222	781	4	195.25
26S protease regulatory subunit 6B	P43686	418	2	209.00
Fragile X mental retardation 1 (FMR-1) (FMRP)	Q06787	632	3	210.67
DNA replication licensing factor MCM4	P33991	863	4	215.75
Hexokinase, type I	P19367	917	4	229.25
DNA replication licensing factor MCM7	P33993	719	3	239.67
CaM-kinase II delta chain	Q13557	499	2	249.50
Flightless-I protein homolog	Q13045	1269	5	253.80
6-phosphofructokinase, liver	P17858	780	3	260.00
DNA replication licensing factor MCM3	P25205	808	3	269.33
β-COP	P53618	953	3	317.67
CD2-associated protein (Cas-SH3 domains)	Q9Y5K6	639	2	319.50
Protein disulfide isomerase A4 precursor (ERp72)	P13667	645	2	322.50
Cullin homolog 4A (CUL-4A)	Q13619	659	2	329.50
Vesicle-fusing ATPase	P46459	744	2	372.00
Inhibitor of nuclear factor kappa B kinase beta	O14920	756	2	378.00
gamma-COP	Q9Y678	874	2	437.00
alpha-COP	P53621	1224	2	612.00

*Accession number from the National Center for Biotechnology Information protein database.
†The number of MS peptides recovered matching identified protein.
‡Protein length divided by the number of MS peptides as an approximation of coverage.

Table 3. Functional Assessment of Ezrin N-terminal Binding Proteins Identified by Affinity Chromatography and MS-MS.

Term	*P*	Adjusted *P* (FDR = 0.05)
GO molecular function (levels 4-9)		
Unfolded protein binding (GO:0051082)	2.65*e* – 11	2.44*e* – 08
Actin binding (GO:0003779)	1.46*e* – 09	6.72*e* – 07
Magnesium chelatase activity (GO:0016851)	1.93*e* – 06	1.98*e* – 04
GTPase activity (GO:0003924)	4.54*e* – 06	3.81*e* – 04
GTP binding (GO:0005525)	1.25*e* – 05	9.65*e* – 04
Translation initiation factor activity (GO:0003743)	1.90*e* – 05	1.35*e* – 03
Cadherin binding (GO:0045296)	1.49*e* – 04	9.83*e* – 03
Ribose phosphate diphosphokinase activity (GO:0004749)	3.35*e* – 04	1.93*e* – 02
Protein C-terminus binding (GO:0008022)	9.73*e* – 04	4.82*e* – 02
ATPase activity (GO:0016887)	9.92*e* – 04	4.82*e* – 02
Protein N-terminus binding (GO:0047485)	9.33*e* – 04	4.82*e* – 02
GO cellular component (levels 4-9)		
Actin cytoskeleton (GO:0015629)	2.81*e* – 10	6.43*e* – 08
Filopodium (GO:0030175)	1.20*e* – 08	1.38*e* – 06
Microvillus (GO:0005902)	4.18*e* – 08	3.19*e* – 06
Ruffle (GO:0001726)	1.29*e* – 07	4.99*e* – 06
Cytoplasmic membrane-bounded vesicle (GO:0016023)	3.89*e* – 07	1.27*e* – 05
Cytoskeletal part (GO:0044430)	8.09*e* – 07	2.06*e* – 05
Cytosolic part (GO:0044445)	1.16*e* – 06	2.42*e* – 05
Proteasome complex (GO:0000502)	4.24*e* – 05	8.08*e* – 04
Myofibril (GO:0030016)	6.23*e* – 05	1.10*e* – 03
Endomembrane system (GO:0012505)	8.10*e* – 05	1.24*e* – 03
Soluble fraction (GO:0005625)	1.60*e* – 04	2.16*e* – 03
Perinuclear region of cytoplasm (GO:0048471)	1.83*e* – 04	2.33*e* – 03
Uropod (GO:0001931)	5.00*e* – 04	6.03*e* – 03
Sarcolemma (GO:0042383)	5.39*e* – 04	6.17*e* – 03
Membrane coat (GO:0030117)	6.41*e* – 04	6.99*e* – 03
Apical plasma membrane (GO:0016324)	8.75*e* – 04	9.11*e* – 03
Eukaryotic translation initiation factor 4F complex (GO:0016281)	1.19*e* – 03	1.18*e* – 02
Sarcoplasmic reticulum (GO:0016529)	1.53*e* – 03	1.46*e* – 02
Extrinsic to membrane (GO:0019898)	2.09*e* – 03	1.84*e* – 02
Cytoplasmic vesicle part (GO:0044433)	2.65*e* – 03	2.25*e* – 02
Eukaryotic translation initiation factor 3 complex (GO:0005852)	3.38*e* – 03	2.77*e* – 02
Chloride channel complex (GO:0034707)	3.69*e* – 03	2.91*e* – 02
Dendritic shaft (GO:0043198)	4.87*e* – 03	3.60*e* – 02
Polysome (GO:0005844)	4.87*e* – 03	3.60*e* – 02
Small nucleolar ribonucleoprotein complex (GO:0005732)	5.42*e* – 03	3.88*e* – 02
Cell projection membrane (GO:0031253)	5.99*e* – 03	4.16*e* – 02
GO biological processes (levels 4-9)		
Intracellular protein transport (GO:0006886)	5.00*e* – 09	4.05*e* – 06
Protein folding (GO:0006457)	2.87*e* – 08	1.55*e* – 05
Regulation of cytoskeleton organization (GO:0051493)	8.74*e* – 07	1.88*e* – 04
Regulation of actin polymerization or depolymerization (GO:0008064)	1.24*e* – 06	2.36*e* – 04
Actin filament polymerization (GO:0030041)	1.52*e* – 06	2.36*e* – 04
Negative regulation of ubiquitin-protein ligase activity during mitotic cell cycle (GO:0051436)	3.15*e* – 06	3.82*e* – 04
Positive regulation of ubiquitin-protein ligase activity during mitotic cell cycle (GO:0051437)	4.04*e* – 06	4.15*e* – 04
Actin polymerization or depolymerization (GO:0008154)	6.46*e* – 06	5.72*e* – 04
DNA replication initiation (GO:0006270)	1.28*e* – 05	9.85*e* – 04
Golgi vesicle budding (GO:0048194)	3.11*e* – 05	2.09*e* – 03
Vesicle targeting, to, from or within Golgi (GO:0048199)	4.12*e* – 05	2.69*e* – 03
Negative regulation of protein complex assembly (GO:0031333)	5.06*e* – 05	3.21*e* – 03
Actin filament bundle formation (GO:0051017)	7.81*e* – 05	4.67*e* – 03
Negative regulation of protein complex disassembly (GO:0043242)	9.53*e* – 05	5.55*e* – 03
Small GTPase-mediated signal transduction (GO:0007264)	1.62*e* – 04	8.94*e* – 03
Retrograde vesicle-mediated transport, Golgi to ER (GO:0006890)	2.06*e* – 04	1.09*e* – 02
Regulation of protein complex disassembly (GO:0043244)	2.25*e* – 04	1.13*e* – 02
Membrane to membrane docking (GO:0022614)	3.35*e* – 04	1.60*e* – 02
Negative regulation of cellular component movement (GO:0051271)	4.21*e* – 04	1.89*e* – 02
Regulation of proton transport (GO:0010155)	5.00*e* – 04	2.20*e* – 02
Vesicle organization (GO:0016050)	5.72*e* – 04	2.42*e* – 02
Nucleocytoplasmic transport (GO:0006913)	6.63*e* – 04	2.60*e* – 02
Striated muscle contraction (GO:0006941)	7.57*e* – 04	2.86*e* – 02
Modification-dependent protein catabolic process (GO:0019941)	8.43*e* – 04	3.13*e* – 02
Regulation of defense response to virus by virus (GO:0050690)	9.26*e* – 04	3.38*e* – 02
Body fluid secretion (GO:0007589)	1.02*e* – 03	3.61*e* – 02
Negative regulation of coagulation (GO:0050819)	1.31*e* – 03	4.48*e* – 02

may represent a functionally important multiprotein complex associated with translation.

To demonstrate that Ezrin cosedimentation with translation components was not the result of interaction with nonrelated complexes of a similar density, we treated lysates with EDTA before loading on to sucrose density gradients. EDTA treatment chelates magnesium, a necessary cofactor for ribosomal subunit integrity. As expected, EDTA treatment caused a dramatic decrease in polysomes while

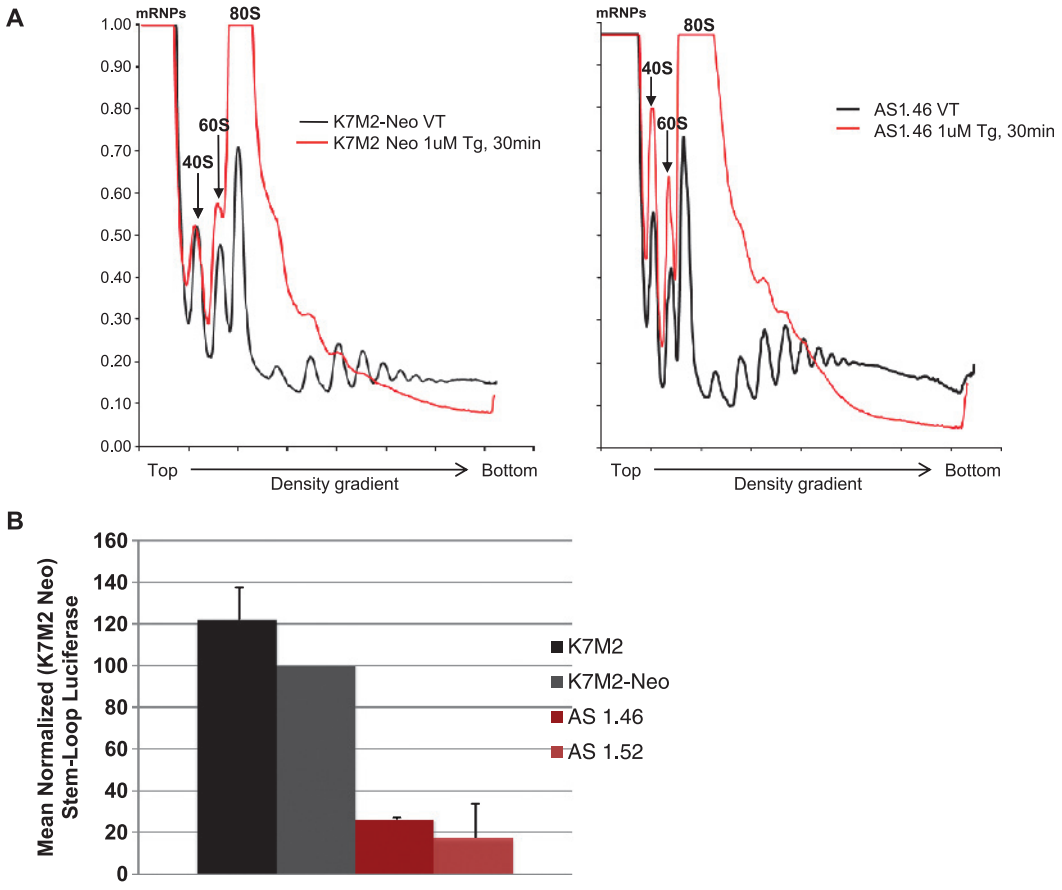

Figure 2. Ezrin expression does not influence global protein translation but contributes to the expression of complex mRNAs. (A) Polysome analysis of high- (K7M2) and low- (AS 1.46) Ezrin-expressing cells was undertaken to assess active protein translation in cells. Cell lysates were then layered onto 15% to 45% linear sucrose gradients for polysome analysis. Samples were fractionated and UV absorbance was measured in real time (black line). The location of 40S and 60S ribosomal subunits as well as 80S ribosome monomers and larger MW polysomes are resolved. Global inhibition of protein translation was observed after treatment of K7M2-WT cells with thapsigargin (Tg 1 μM; red line). (B) Ezrin expression enhances expression of a synthetic protein (luciferase reporter) with a complex 5′UTR. High- (K7M2 and K7M2-Neo) and low- (AS 1.46 and AS 1.52) metastatic/Ezrin-expressing murine OS cells were transfected with a construct designed to represent a cap-dependent "weakly translated" protein with a complex 5′ untranslated region adjacent to the reporter fLUC gene (pcDNA-SL-LUC). Data represent mean normalized luciferase units (normalized to K7M2-neo) from five distinct reporter experiments.

promoting a concomitant increase in the levels of dissociated ribosomal subunits (Figure 3*B*). In addition, Ezrin protein levels, along with RACK1, decreased in 40S fractions. This suggested that cosedimentation of Ezrin in 40S fractions of non–EDTA-treated samples (Figure 3*A*) was dependent on intact ribosomes, indicating that Ezrin may be a part of the translation preinitiation complex. To investigate this possibility, we used an approach to enrich for functional, cap-bound translation initiation factors in K7M2 OS cell lysates. Alterations in protein translation are often mediated by the expression and availability of eukaryotic translation initiation factors, such as eIF4E, or as a result of alterations in the regulation of signaling pathways. eIF4E binds to the 7-methylguanosine "cap" present at the 5′ end of all eukaryotic mRNAs and is central to formation of the translation preinitiation complex. As shown in Figure 3*C*, eIF4E, was efficiently captured from tumor cell lysates as were eIF4G and 4E-BP1. However, we were unable to detect the binding of Ezrin, or other ERM family members using this approach. These results show that, although Ezrin cosediments with factors involved in translation initiation, there is no direct interaction of Ezrin and cap-bound proteins. We next asked if Ezrin might interact with proteins that may stabilize the translational loop structure at the 3′ UTR of complex proteins. Indeed, we found a direct interaction between Ezrin and the poly A binding protein (PABP1; Figure 3, *D* and *E*). In support of the interaction between PABP1 and Ezrin, the use of small molecules that directly bind to Ezrin and inhibit metastasis *in vivo* also blocked the interaction between PABP1 and Ezrin (Figure 3*F*) [19]. Collectively, these findings provide new insights into the association of Ezrin with the ribonucleoprotein complex and may suggest a role for Ezrin in the stabilization of the translational machinery during its interaction with mRNA early during the initiation or regulation of translation. Our data do not support a role for Ezrin in active and ongoing mRNA translation.

The Cellular Relevance of Enhanced Protein Translation in Metastatic Cells

The active, phosphorylated form of Ezrin is enriched at the cell membrane, and it regulates signaling dynamics associated with actin reorganization during cell motility [18]. To determine whether components of the translation machinery colocalized with active Ezrin/ERM family proteins in this context, we purified pseudopodia from

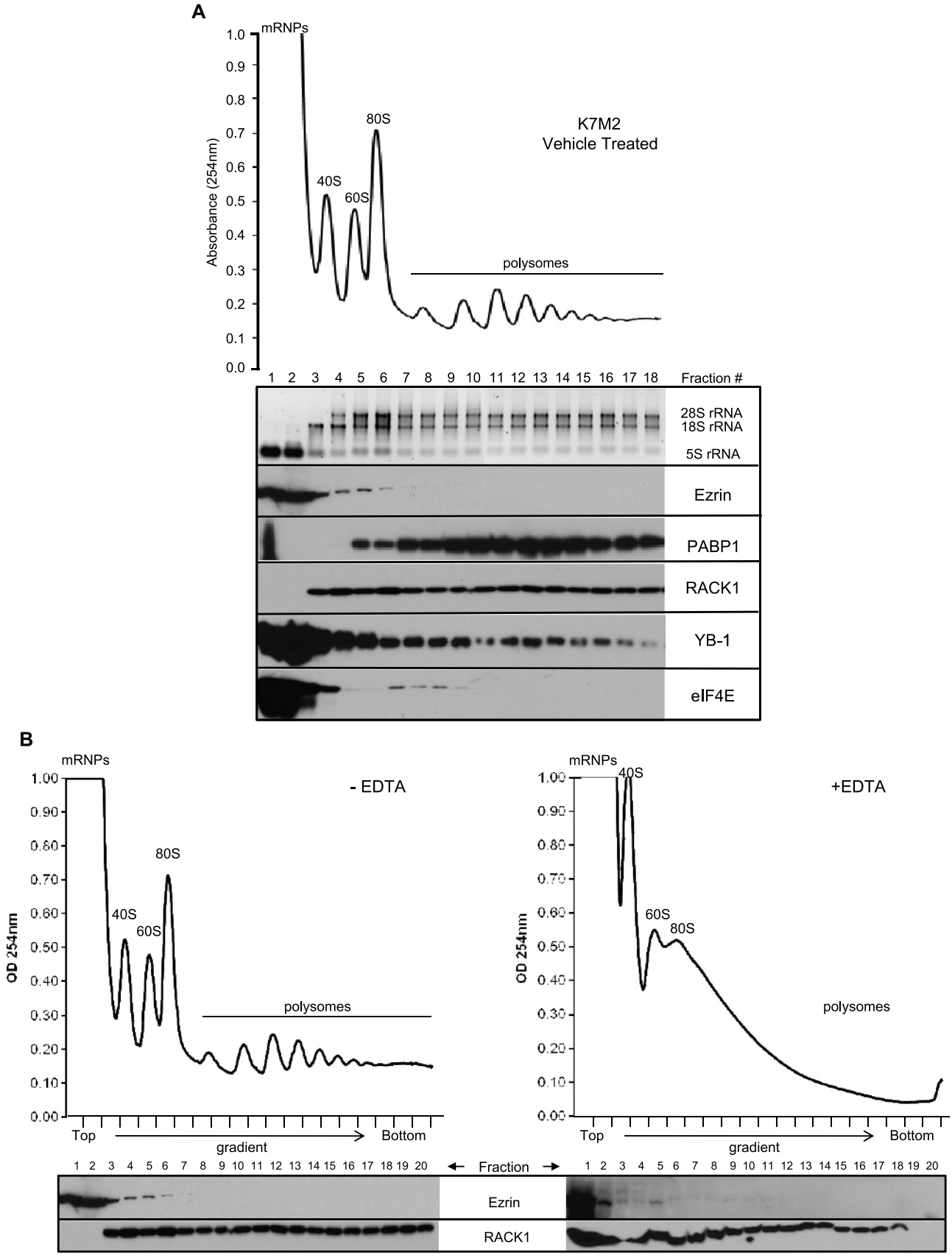
A
mRNPs
80S
40S
60S
K7M2
Vehicle Treated
Absorbance (254nm)
polysomes
1 2 3 4 5 6 7 8 9 10 11 12 13 14 15 16 17 18 Fraction #
28S rRNA
18S rRNA
5S rRNA
Ezrin
PABP1
RACK1
YB-1
eIF4E
B
mRNPs
- EDTA
80S
40S
60S
polysomes
OD 254nm
Top
gradient
Bottom
1 2 3 4 5 6 7 8 9 10 11 12 13 14 15 16 17 18 19 20
Fraction
mRNPs
40S
+EDTA
60S
80S
polysomes
Top
gradient
Bottom
1 2 3 4 5 6 7 8 9 10 11 12 13 14 15 16 17 18 19 20
Ezrin
RACK1

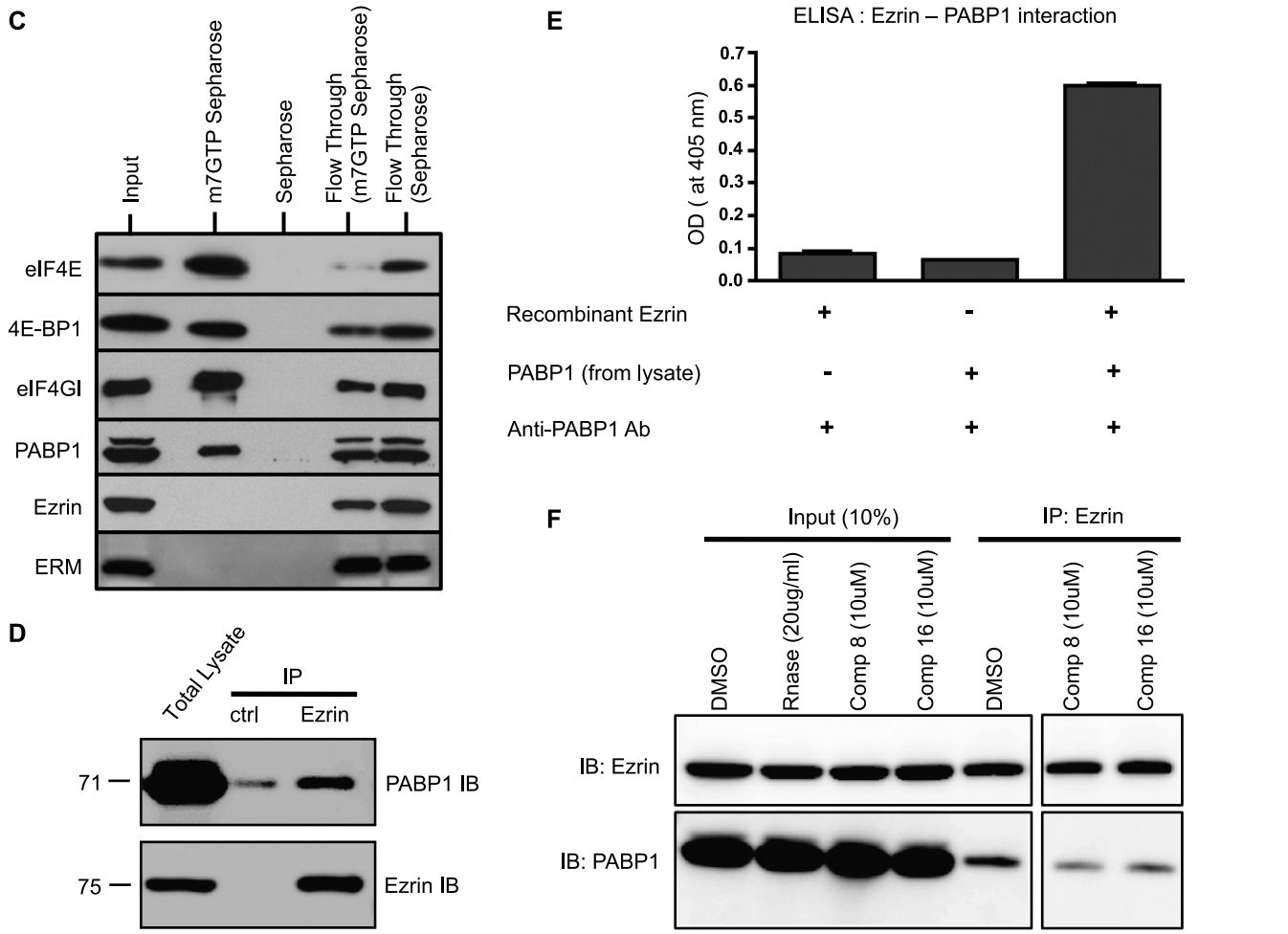

Figure 3. (*continued*).

migrating OS cells. Cells were plated on collagen/laminin–coated membranes containing 0.2-μm pores. This selective pore size allows invasion of pseudopod extensions through the pores in response to a chemotactic gradient (e.g., high serum) while excluding cell bodies. Western blot analysis was then undertaken for Ezrin and other proteins involved in protein translation from invading pseudopodia (extracted from the lower part of the membrane) or cell bodies (extracted from the upper part of the membrane) of metastatic human and murine

Figure 3. Ezrin cosediments with messenger ribonucleoprotein (mRNP) complexes, ribosomal subunits and also interacts with PABP1. (A) Ezrin is part of the ribonucleoprotein complex. Sucrose density gradient centrifugation was used to isolate and resolve messenger ribonucleoprotein complexes. Western blot was used to determine the presence of Ezrin and other proteins known to be part of the translational machinery in fractions spanning the entire gradient. Consistent with its role in translational initiation eIF4E was detected mainly in fractions containing free mRNPs and 40S-80S complexes. RACK1, a core ribosome binding protein, was found in fractions containing ribosomal subunits, monosomes, or polysomes and was not detectable in the free mRNP fractions. YB-1 was enriched in polysome fractions consistent with its role as an mRNA binding protein. Ezrin was distributed mainly in free mRNP fractions (similar to that of eIF4E) but also in smaller amounts with 40S, 60S, and monosomes. ERM family members including Ezrin showed a similar overlapping pattern of protein migration (not shown). Polysome lysates were then dissociated with 25 mM EDTA treatment before loading on sucrose density gradients. (B) EDTA treatment resulted in ribonucleoprotein dissociation. (C) Ezrin is not enriched in 5′ methyl cap binding complex. An affinity matrix composed of 7-methyl-GTP covalently linked to sepharose beads was used to determine whether Ezrin associates with the cap-binding structure. eIF4E and known eIF4E interacting proteins such as PABP1, eIF4G, and 4E-BP1 were efficiently pulled down. Ezrin and other ERM family members were not found to be enriched with the cap binding complex. (D) Ezrin interacts with the 3′ binding protein PABP1. Western blot immunoprecipitation demonstrated a direct interaction between Ezrin and PABP1. (E) ELISA plate wells were coated with recombinant Ezrin. K12 cell lysate was used as the source of PABP1 protein. Ezrin-PABP1 complexes were detected using anti-PABP1 antibody. A meaningful signal was observed only in the presence of both Ezrin and PABP1. Experiments were performed twice in triplicates and a representative result is shown. Graph represents the average of triplicate readings with error bars indicating SD. (F) Ezrin-containing protein complexes in K7M2 cells were immunoprecipitated with an anti-Ezrin antibody. The presence of PABP1 in this complex was confirmed by Western blot. Two small molecules, previously defined by their ability to bind Ezrin and interrupt its interactions with other proteins [19], compound 8 (NSC305787) and compound 16 (NSC668394), blocked the interaction between Ezrin and PABP1 compared with vehicle (DMSO)-treated condition without affecting immunoprecipitation efficiency.

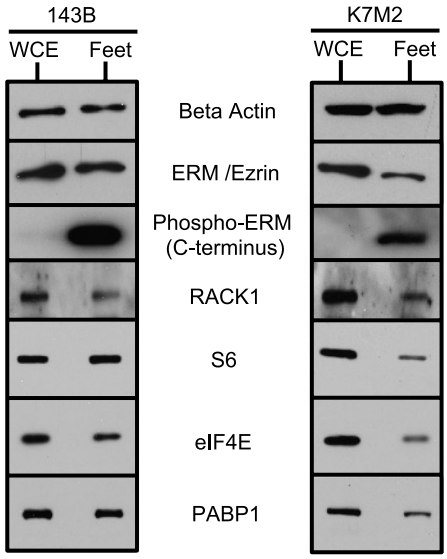

Figure 4. Active Ezrin and elements of the translational machinery are present in invading pseudopodia. Migrating highly metastatic human and murine OS cells (143B and K7M2, respectively) were plated on collagen/laminin–coated membranes containing 0.2-μm pores. Lysates collected from the whole cell body (WCE) and invading pseudopodia (feet) were collected. Western blot analysis demonstrated expression of Ezrin and proteins involved in protein translation in these invading cellular structures.

OS cells (Figure 4). Samples were normalized so that equal amounts of protein were loaded for each condition. As expected, phosphorylated ERM family proteins were enriched in migrating pseudopodia. The relative levels of total ERM (unphosphorylated) protein were similar to the cell bodies. Interestingly ribosomal S6, the 40S core protein, RACK1, and eIF4E (proteins needed for the initiation of translation) were all found in these invading pseudopodia. Levels of β-actin were similar in both fractions. These data support the hypothesis that, during metastatic progression, Ezrin may provide efficiency to metastatic cells by allowing the translation of needed proteins at distinct points in time and in distinct subcellular localizations (i.e., invadapodia). A corollary of this hypothesis is that the inability of nonmetastatic cells to deliver these needed proteins prevents them from successfully metastasizing.

Discussion

We previously identified the cytoskeleton linker protein, Ezrin, as part of our effort to expand our understanding of the biology of metastasis in pediatric sarcomas [1,20]. Since then, several groups have identified associations between Ezrin expression and clinical outcome in a variety of human cancers [9,36–40]. We previously hypothesized that Ezrin enhances the ability of metastatic cells to endure specific stresses related to metastatic progression [1]. The inefficiency of metastasis is believed to be primarily influenced by an inability of the majority of cancer cells to manage stresses that are faced after cells arrive at distant secondary sites. High-Ezrin-expressing cells are better able to resist this inefficiency early during progression at secondary sites [41]. From these data, we hypothesized that Ezrin expression allowed cells to rapidly adapt to the foreign lung microenvironment and manage cellular stresses. However, it has been unclear how Ezrin provided this advantage during the process of metastasis. To address this question, we used two non-candidate approaches to identify biologic processes affected by Ezrin in OS cells. First, a genomic comparison of high- and low-Ezrin-expressing OS cells resulted in a transcriptional signature of 181 genes that correlated with high Ezrin expression. Functional analysis of these cDNAs revealed unexpected enrichment of gene functions related to protein biosynthesis. In parallel, we used affinity chromatography in which the N-terminus of Ezrin was used to capture putative Ezrin-interacting proteins present in tumor extracts. A total of 138 bound proteins were identified by tandem mass spectrometry and surprisingly, we again found enrichment of proteins associated with protein translation and the translational machinery. These included known RNA-binding proteins, translation initiation factors, the core 40S ribosomal subunit protein, RACK1, and the 3′ mRNA binding protein, PABP1. Previous studies have demonstrated that cytoskeletal dynamics and translation may be coregulated [42–46]. Furthermore, to our knowledge, our study is the first to associate Ezrin with protein translation and with elevated expression of components of the translation machinery such as eIF4E.

Because eIF4E binding to the 5′ cap of cellular mRNA is considered a major rate-limiting step in protein synthesis, increased expression in the presence of Ezrin may provide a means for enhanced anabolic processes such as tumor cell growth. Increased expression of eIF4E has been shown to enhance translation of mRNA with a complex, highly structured 5′ untranslated region [29]. Consistent with this idea, expression of a weakly translated stem-loop reporter was increased in high-Ezrin-expressing cells. We considered the possibility that enhanced translation may be a general phenomenon affecting global rates of protein synthesis. However, quantitative polysome analysis of steady-state translation levels failed to reveal differences between high- and low-Ezrin-expressing cells. In addition, polysome profiles from physiologically stressed cells were also similar regardless of Ezrin levels. Taken together, these data suggested that Ezrin might have an effect on the translation of specific mRNAs with complex 5′ untranslated regions rather than on global protein synthesis. This may not be surprising because both high- and low-Ezrin-expressing OS cells are viable, proliferate *in vitro* and yield similar primary tumor growth features *in vivo*. The distinction among these cells is the inability of cells with low Ezrin to metastasize [1]. A model of selective protein translation describes proteins as either "strongly translated" or "weakly translated" [47]. The strongly translated proteins undergo very limited regulation of translation, whereas the "weakly translated proteins" are largely maintained as stable mRNAs and await cues that activate the translational machinery to translate these complex proteins [48]. Common among such "weakly translated proteins" is complexity in the 5′ and 3′ untranslated regions. Because it is energetically impossible to express all proteins at all times, this proposed model suggests that cells in dynamic environments activate the translational machinery in times of need; as such, these "weakly translated proteins" undergo translation only when they are most needed. Examples of "weakly translated proteins" include proteins involved in acute phase responses and several oncogenes [49].

Extending this hypothesis, we next asked whether Ezrin and components of the translational machinery were present in subcellular locations relevant to metastasis such as invading pseudopodia. Indeed, we demonstrated the presence of phosphorylated forms of Ezrin, and critical parts of the translational machinery (i.e., RACK1, eIF4E) are present in these invading pseudopodia. These studies support the notion that enhanced efficiency of metastasis may not be limited to a kinetic advantage alone but may also involve the

opportunity to deliver proteins in the areas of greatest need during metastasis. It is attractive to consider the dynamic needs of highly metastatic cells and an efficiency in metastasis being conferred on cells that are able to meet these needs through the delivery of necessary proteins at specific times and locations within the cell [29]. Previous studies have shown that actin dynamics can alter translation by directly affecting both transport of specific mRNA within the cell as well as signaling to and from the protein synthesis machinery [45]. For example, during development, axons become polarized, migrating in response to chemotactic gradients. During this migration, transmembrane receptors in the growth cone become activated stimulating formation of actin-rich filopodia and lamellipodia. In this context, the cytoskeleton serves as a scaffold for RNA binding proteins, translation factors, and signaling intermediates, enabling the spatiotemporal regulation of protein synthesis [50]. In light of our current data and given the classic role of Ezrin as an actin-binding protein, one can envision that a similar scenario may occur in migrating and invading tumor cells during metastatic progression.

In further support of the link between Ezrin and protein translation, sucrose density gradient fractionation of whole cell lysates revealed that a portion of total Ezrin protein was present in fractions containing the RNA binding proteins YB-1 and PABP1 as well as the cap binding protein eIF4E and RACK1. These results provided a functional context in which the majority of Ezrin was present in free mRNP fractions, whereas a smaller portion was present in "lighter" ribosomal units. The absence of Ezrin in more heavily weighted polysomes suggested a role for Ezrin in the early phases of protein synthesis such as mRNA transport, formation of the preinitiation complex, or initiation rather than elongation or termination. These possibilities were further narrowed down after we failed to detect the presence of Ezrin using 7-methyl guanosine cap affinity chromatography to functionally enrich for components of the cap-binding complex. In addition, eIF4A, eIF4G, and eIF4E were all absent from Ezrin immunoprecipitates (data not shown). However, one protein, identified by MS-MS, that did coimmunoprecipitate with Ezrin was poly-A binding protein (PABP1). Similar results have been seen for binding of paxillin to PABP1 [50]. In addition, paxillin/PABP1 complexes demonstrate nucleocytoplasmic shuttling in a CRM1-dependent manner [51]. There have been some reports of Ezrin localizing to the nucleus, and it is interesting to speculate that PABP1 may play a role in nucleocytoplasmic shuttling of Ezrin as well [52,53]. Although we cannot conclude from our current studies whether Ezrin/PABP1 interaction is responsible for Ezrin's role in translation and metastasis, we have identified small molecule inhibitors, which block their interaction and, importantly, also inhibit metastatic progression *in vivo* [19]. Having established this phenotypic relevance, studies are under way to characterize the nature of Ezrin/PABP1 interaction including the dynamics and subcellular localization. In addition, future studies will be aimed at identifying those endogenous mRNA, which may coassociate with Ezrin/PABP1, specifically those with complex 5′UTR as candidates for enhanced translation and which contribute to metastasis.

Collectively, these data provide support for a broader complex of proteins that may collectively contribute to efficient protein translation. In our current report, we found that Ezrin interacts with RACK1, by Ezrin affinity chromatography and cofractionation with a portion of endogenous Ezrin in sucrose density gradient analysis. A wealth of electron microscopy and crystal structure data have established the location of RACK1 binding to the 40S ribosomal subunit and functional analysis has revealed that RACK1 serves as a docking site and scaffold for multiple proteins, including PABP1 and protein kinase C (PKC), which regulate translation [33,54–56]. Interestingly, we have previously shown that PKC isoforms coimmunoprecipitate with Ezrin and mediate C-terminal Ezrin phosphorylation, believed to regulate Ezrin's activation in OS cells [18]. We hypothesize that a complex involving Ezrin, PABP1, and PKC with close interaction with RACK1 would be well positioned to efficiently regulate the translational machinery in response to the stresses of metastasis.

Based on a confluence of functional data from genomic and proteomic assessment of Ezrin function, we generated a hypothesis that Ezrin contributes to the efficiency of metastasis by enhancing the process of protein translation. In support of this hypothesis, we demonstrated that Ezrin is part of the ribonucleoprotein complex, interacts with PABP1, and may enhance the translation of specific proteins at specific subcellular locations, critical to the metastatic phenotype. A potential clinical impact of these findings is a biologic rationale for the use of inhibitors of translation initiation, such as rapamycin and related synthetic analogs, in the context of metastatic progression rather than solely for established disease. Collectively, these data support new functions for Ezrin in the metastatic phenotype of cancer and serve as a foundation for studies that will elucidate the mechanisms by which this occurs.

References

[1] Khanna C, Wan X, Bose S, Cassaday R, Olomu O, Mendoza A, Yeung C, Gorlick R, Hewitt SM, and Helman LJ (2004). The membrane-cytoskeleton linker ezrin is necessary for osteosarcoma metastasis. *Nat Med* **10**, 182–186.

[2] Yu Y, Khan J, Khanna C, Helman L, Meltzer PS, and Merlino G (2004). Expression profiling identifies the cytoskeletal organizer ezrin and the developmental homeoprotein Six-1 as key metastatic regulators. *Nat Med* **10**, 175–181.

[3] Ilmonen S, Vaheri A, Asko-Seljavaara S, and Carpen O (2005). Ezrin in primary cutaneous melanoma. *Mod Pathol* **18**, 503–510.

[4] Ohtani K, Sakamoto H, Rutherford T, Chen Z, Satoh K, and Naftolin F (1999). Ezrin, a membrane-cytoskeletal linking protein, is involved in the process of invasion of endometrial cancer cells. *Cancer Lett* **147**, 31–38.

[5] Pang ST, Fang X, Valdman A, Norstedt G, Pousette A, Egevad L, and Ekman P (2004). Expression of ezrin in prostatic intraepithelial neoplasia. *Urology* **63**, 609–612.

[6] Tokunou M, Niki T, Saitoh Y, Imamura H, Sakamoto M, and Hirohashi S (2000). Altered expression of the ERM proteins in lung adenocarcinoma. *Lab Invest* **80**, 1643–1650.

[7] Tynninen O, Carpen O, Jaaskelainen J, Paavonen T, and Paetau A (2004). Ezrin expression in tissue microarray of primary and recurrent gliomas. *Neuropathol Appl Neurobiol* **30**, 472–477.

[8] Weng WH, Ahlen J, Astrom K, Lui WO, and Larsson C (2005). Prognostic impact of immunohistochemical expression of ezrin in highly malignant soft tissue sarcomas. *Clin Cancer Res* **11**, 6198–6204.

[9] Bruce B, Khanna G, Ren L, Landberg G, Jirstrom K, Powell C, Borczuk A, Keller ET, Wojno KJ, Meltzer P, et al. (2007). Expression of the cytoskeleton linker protein ezrin in human cancers. *Clin Exp Metastasis* **24**, 69–78.

[10] Reczek D, Berryman M, and Bretscher A (1997). Identification of EBP50: a PDZ-containing phosphoprotein that associates with members of the ezrin-radixin-moesin family. *J Cell Biol* **139**, 169–179.

[11] Tsukita S, Oishi K, Sato N, Sagara J, and Kawai A (1994). ERM family members as molecular linkers between the cell surface glycoprotein CD44 and actin-based cytoskeletons. *J Cell Biol* **126**, 391–401.

[12] Berryman M, Franck Z, and Bretscher A (1993). Ezrin is concentrated in the apical microvilli of a wide variety of epithelial cells whereas moesin is found primarily in endothelial cells. *J Cell Sci* **105**(pt 4), 1025–1043.

[13] Bretscher A, Chambers D, Nguyen R, and Reczek D (2000). ERM-Merlin and EBP50 protein families in plasma membrane organization and function. *Annu Rev Cell Dev Biol* **16**, 113–143.

[14] Wu KL, Khan S, Lakhe-Reddy S, Jarad G, Mukherjee A, Obejero-Paz CA, Konieczkowski M, Sedor JR, and Schelling JR (2004). The NHE1 Na^+/H^+ exchanger recruits ezrin/radixin/moesin proteins to regulate Akt-dependent cell survival. *J Biol Chem* **279**, 26280–26286.

[15] Bretscher A, Edwards K, and Fehon RG (2002). ERM proteins and merlin: integrators at the cell cortex. *Nat Rev Mol Cell Biol* **3**, 586–599.

[16] Ng T, Parsons M, Hughes WE, Monypenny J, Zicha D, Gautreau A, Arpin M, Gschmeissner S, Verveer PJ, Bastiaens PI, et al. (2001). Ezrin is a downstream effector of trafficking PKC-integrin complexes involved in the control of cell motility. *EMBO J* **20**, 2723–2741.

[17] Serrador JM, Nieto M, and Sanchez-Madrid F (1999). Cytoskeletal rearrangement during migration and activation of T lymphocytes. *Trends Cell Biol* **9**, 228–233.

[18] Ren L, Hong SH, Cassavaugh J, Osborne T, Chou AJ, Kim SY, Gorlick R, Hewitt SM, and Khanna C (2009). The actin-cytoskeleton linker protein ezrin is regulated during osteosarcoma metastasis by PKC. *Oncogene* **28**, 792–802.

[19] Bulut G, Hong SH, Chen K, Beauchamp EM, Rahim S, Kosturko GW, Glasgow E, Dakshanamurthy S, Lee HS, Daar I, et al. (2012). Small molecule inhibitors of ezrin inhibit the invasive phenotype of osteosarcoma cells. *Oncogene* **31**, 269–281.

[20] Khanna C, Khan J, Nguyen P, Prehn J, Caylor J, Yeung C, Trepel J, Meltzer P, and Helman L (2001). Metastasis-associated differences in gene expression in a murine model of osteosarcoma. *Cancer Res* **61**, 3750–3759.

[21] Bretscher A, Reczek D, and Berryman M (1997). Ezrin: a protein requiring conformational activation to link microfilaments to the plasma membrane in the assembly of cell surface structures. *J Cell Sci* **110**(pt 24), 3011–3018.

[22] Yang HS, Cho MH, Zakowicz H, Hegamyer G, Sonenberg N, and Colburn NH (2004). A novel function of the MA-3 domains in transformation and translation suppressor Pdcd4 is essential for its binding to eukaryotic translation initiation factor 4A. *Mol Cell Biol* **24**, 3894–3906.

[23] Wei JS and Khan J (2002). *Purification of Total RNA from Mammalian Cells and Tissue*. Cold Spring Harbor Laboratory Press, New York, NY.

[24] Son CG, Bilke S, Davis S, Greer BT, Wei JS, Whiteford CC, Chen QR, Cenacchi N, and Khan J (2005). Database of mRNA gene expression profiles of multiple human organs. *Genome Res* **15**, 443–450.

[25] Riss J, Khanna C, Koo S, Chandramouli GV, Yang HH, Hu Y, Kleiner DE, Rosenwald A, Schaefer CF, Ben-Sasson SA, et al. (2006). Cancers as wounds that do not heal: differences and similarities between renal regeneration/repair and renal cell carcinoma. *Cancer Res* **66**, 7216–7224.

[26] Gotz S, Garcia-Gomez JM, Terol J, Williams TD, Nagaraj SH, Nueda MJ, Robles M, Talon M, Dopazo J, and Conesa A (2008). High-throughput functional annotation and data mining with the Blast2GO suite. *Nucleic Acids Res* **36**, 3420–3435.

[27] Reczek D and Bretscher A (1998). The carboxyl-terminal region of EBP50 binds to a site in the amino-terminal domain of ezrin that is masked in the dormant molecule. *J Biol Chem* **273**, 18452–18458.

[28] Wilm M, Shevchenko A, Houthaeve T, Breit S, Schweigerer L, Fotsis T, and Mann M (1996). Femtomole sequencing of proteins from polyacrylamide gels by nano-electrospray mass spectrometry. *Nature* **379**, 466–469.

[29] Graff JR and Zimmer SG (2003). Translational control and metastatic progression: enhanced activity of the mRNA cap-binding protein eIF-4E selectively enhances translation of metastasis-related mRNAs. *Clin Exp Metastasis* **20**, 265–273.

[30] Parsyan A, Svitkin Y, Shahbazian D, Gkogkas C, Lasko P, Merrick WC, and Sonenberg N (2011). mRNA helicases: the tacticians of translational control. *Nat Rev Mol Cell Biol* **12**, 235–245.

[31] Sehgal A, Briggs J, Rinehart-Kim J, Basso J, and Bos TJ (2000). The chicken c-Jun 5′ untranslated region directs translation by internal initiation. *Oncogene* **19**, 2836–2845.

[32] Stoneley M and Willis AE (2003). Aberrant regulation of translation initiation in tumorigenesis. *Curr Mol Med* **3**, 597–603.

[33] Coyle SM, Gilbert WV, and Doudna JA (2009). Direct link between RACK1 function and localization at the ribosome *in vivo*. *Mol Cell Biol* **29**, 1626–1634.

[34] Nilsson J, Sengupta J, Frank J, and Nissen P (2004). Regulation of eukaryotic translation by the RACK1 protein: a platform for signalling molecules on the ribosome. *EMBO Rep* **5**, 1137–1141.

[35] Evdokimova V, Ruzanov P, Anglesio MS, Sorokin AV, Ovchinnikov LP, Buckley J, Triche TJ, Sonenberg N, and Sorensen PH (2006). Akt-mediated YB-1 phosphorylation activates translation of silent mRNA species. *Mol Cell Biol* **26**, 277–292.

[36] Kang YK, Hong SW, Lee H, and Kim WH (2010). Prognostic implications of ezrin expression in human hepatocellular carcinoma. *Mol Carcinog* **49**, 798–804.

[37] Wei YC, Li CF, Yu SC, Chou FF, Fang FM, Eng HL, Uen YH, Tian YF, Wu JM, Li SH, et al. (2009). Ezrin overexpression in gastrointestinal stromal tumors: an independent adverse prognosticator associated with the non-gastric location. *Mod Pathol* **22**, 1351–1360.

[38] Elzagheid A, Korkeila E, Bendardaf R, Buhmeida A, Heikkila S, Vaheri A, Syrjanen K, Pyrhonen S, and Carpen O (2008). Intense cytoplasmic ezrin immunoreactivity predicts poor survival in colorectal cancer. *Hum Pathol* **39**, 1737–1743.

[39] Madan R, Brandwein-Gensler M, Schlecht NF, Elias K, Gorbovitsky E, Belbin TJ, Mahmood R, Breining D, Qian H, Childs G, et al. (2006). Differential tissue and subcellular expression of ERM proteins in normal and malignant tissues: cytoplasmic ezrin expression has prognostic significance for head and neck squamous cell carcinoma. *Head Neck* **28**, 1018–1027.

[40] Kobel M, Gradhand E, Zeng K, Schmitt WD, Kriese K, Lantzsch T, Wolters M, Dittmer J, Strauss HG, Thomssen C, et al. (2006). Ezrin promotes ovarian carcinoma cell invasion and its retained expression predicts poor prognosis in ovarian carcinoma. *Int J Gynecol Pathol* **25**, 121–130.

[41] Wong CW, Lee A, Shientag L, Yu J, Dong Y, Kao G, Al-Mehdi AB, Bernhard EJ, and Muschel RJ (2001). Apoptosis: an early event in metastatic inefficiency. *Cancer Res* **61**, 333–338.

[42] Chicurel ME, Singer RH, Meyer CJ, and Ingber DE (1998). Integrin binding and mechanical tension induce movement of mRNA and ribosomes to focal adhesions. *Nature* **392**, 730–733.

[43] Kim S and Coulombe PA (2010). Emerging role for the cytoskeleton as an organizer and regulator of translation. *Nat Rev Mol Cell Biol* **11**, 75–81.

[44] Polak P, Oren A, Ben-Dror I, Steinberg D, Sapoznik S, Arditi-Duvdevany A, and Vardimon L (2006). The cytoskeletal network controls c-Jun translation in a UTR-dependent manner. *Oncogene* **25**, 665–676.

[45] Van Horck FP and Holt CE (2008). A cytoskeletal platform for local translation in axons. *Sci Signal* **1**, pe11.

[46] Willett M, Flint SA, Morley SJ, and Pain VM (2006). Compartmentalisation and localisation of the translation initiation factor (eIF) 4F complex in normally growing fibroblasts. *Exp Cell Res* **312**, 2942–2953.

[47] De Benedetti A and Graff JR (2004). eIF-4E expression and its role in malignancies and metastases. *Oncogene* **23**, 3189–3199.

[48] Livingstone M, Atas E, Meller A, and Sonenberg N (2010). Mechanisms governing the control of mRNA translation. *Phys Biol* **7**, 021001.

[49] Hsieh AC and Ruggero D (2010). Targeting eukaryotic translation initiation factor 4E (eIF4E) in cancer. *Clin Cancer Res* **16**, 4914–4920.

[50] Woods AJ, Roberts MS, Choudhary J, Barry ST, Mazaki Y, Sabe H, Morley SJ, Critchley DR, and Norman JC (2002). Paxillin associates with poly(A)-binding protein 1 at the dense endoplasmic reticulum and the leading edge of migrating cells. *J Biol Chem* **277**, 6428–6437.

[51] Woods AJ, Kantidakis T, Sabe H, Critchley DR, and Norman JC (2005). Interaction of paxillin with poly(A)-binding protein 1 and its role in focal adhesion turnover and cell migration. *Mol Cell Biol* **25**, 3763–3773.

[52] Di Cristofano C, Leopizzi M, Miraglia A, Sardella B, Moretti V, Ferrara A, Petrozza V, and Della Rocca C (2010). Phosphorylated ezrin is located in the nucleus of the osteosarcoma cell. *Mod Pathol* **23**, 1012–1020.

[53] Batchelor CL, Woodward AM, and Crouch DH (2004). Nuclear ERM (ezrin, radixin, moesin) proteins: regulation by cell density and nuclear import. *Exp Cell Res* **296**, 208–222.

[54] Rabl J, Leibundgut M, Ataide SF, Haag A, and Ban N (2011). Crystal structure of the eukaryotic 40S ribosomal subunit in complex with initiation factor 1. *Science* **331**, 730–736.

[55] Sengupta J, Nilsson J, Gursky R, Spahn CM, Nissen P, and Frank J (2004). Identification of the versatile scaffold protein RACK1 on the eukaryotic ribosome by cryo-EM. *Nat Struct Mol Biol* **11**, 957–962.

[56] Angenstein F, Evans AM, Settlage RE, Moran ST, Ling SC, Klintsova AY, Shabanowitz J, Hunt DF, and Greenough WT (2002). A receptor for activated C kinase is part of messenger ribonucleoprotein complexes associated with polyA-mRNAs in neurons. *J Neurosci* **22**, 8827–8837.

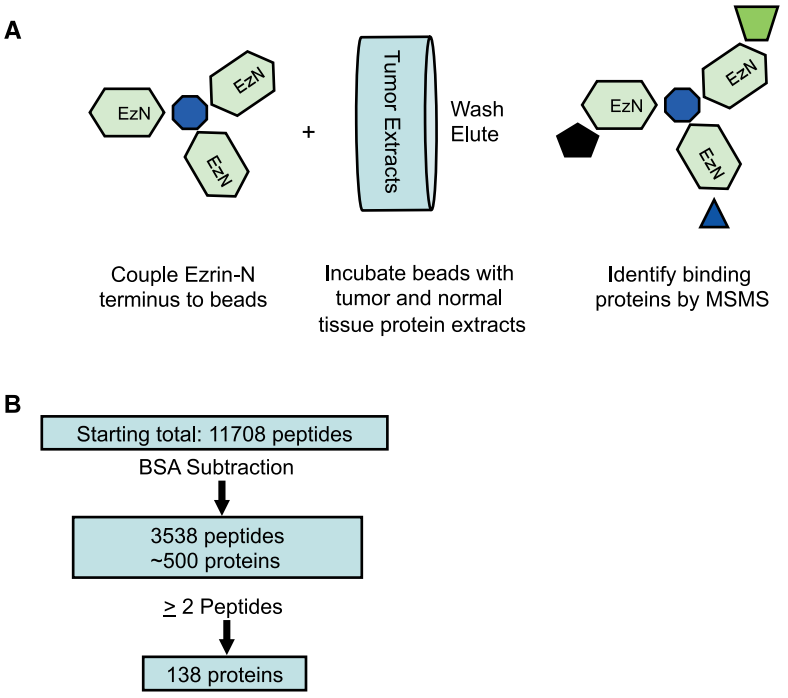

Figure W1. Ezrin-binding proteins resolved by affinity chromatography followed by tandem mass spectrometry. (A) Schematic diagram describing affinity chromatography followed by tandem mass spectrometry approach. N-terminal Ezrin was purified and expressed on sepharose beads. K7M2 murine OS primary tumor and pulmonary metastasis tissue, K7M2 murine OS cell lines, normal mouse lung, and normal mouse muscle were applied to Ezrin beads for affinity chromatography in the presence of ATP. Eluted proteins were then resolved by tandem mass spectrometry. (B) Identification of 138 OS Ezrin-interacting proteins. MS-MS peptides identified in tumor tissue by MS-MS were filtered of nonspecific interacting proteins by BSA subtraction. Further subtraction of proteins was then based the removal of proteins not identified by two or more unique peptides in the MS-MS data.

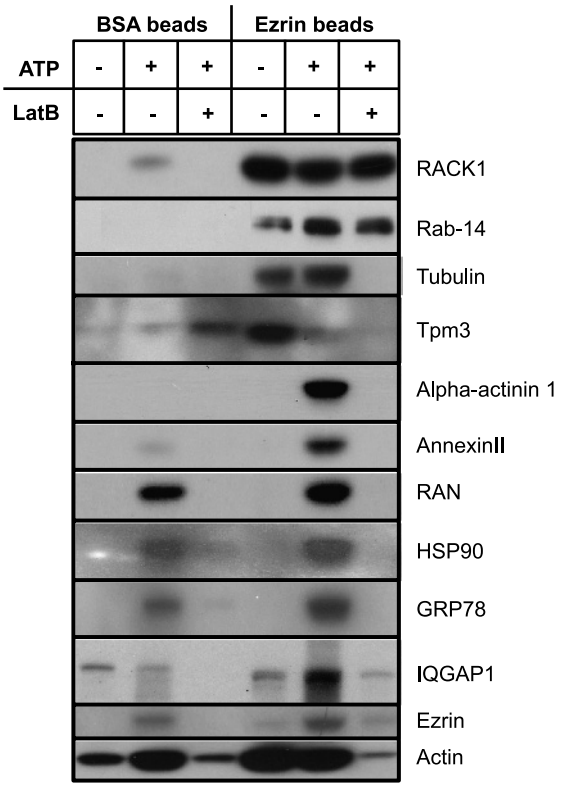

Figure W2. Western blot validation of selected tumor specific proteins identified by Ezrin affinity chromatography. Eluted proteins from BSA and N-terminal Ezrin affinity chromatography were assessed by Western blot before and after the addition of ATP (to optimally open Ezrin conformation) and latrunculin B (for disruption of the actin cytoskeleton). In the absence of ATP, the closed conformation of Ezrin prevails. The majority of identified proteins likely have indirect interactions with Ezrin through the actin cytoskeleton, as supported by the absence of detectable bands for most protein candidates after latrunculin B treatment. Proteins that retained interaction with Ezrin after actin disruption included IQGAP1, Ezrin, RACK1, and Rab 14.